Philippine Engineering Journal (1998) XIX (1): 21-34

HIGHLY ACTIVE ABSORBENT FOR SO_2 REMOVAL PREPARED FROM COAL ASH (PART 1)

K. Nakagawa, K. Yamada, T. Tsurue, S. Takeda and K. Ishizaki
Hokkaido National Industrial Research Institute
Hokkaido, Sapporo, Japan

and

T.A. Quilao, W.A. Balais, A.B. Herrera, D.L. Pugal, H.H. Bion
C.G. Magpantay, F.I. Abarquez, E.M. Alcoba and F.D. Vinluan, Jr.
Fuels and Energy Division
Industrial Technology Development Institute
Bicutan, Taguig, Metro Manila

ABSTRACT

Coal ash samples from Batangas Coal-Fired Thermal Power Plant and limestone from a cement plant in Bulacan were used as raw materials for the preparation of highly active SO_2 absorbent. The prepared SO_2 absorbents were characterized to determine the effects of mineralogical composition, morphological structure and the type of coal ash used, on SO_2 removal efficiency. The desulfurization activity of the SO_2 absorbents were determined by varying the curing conditions and CaO content.

Among the coal ashes, fly ash exhibited the highest SO_2 removal efficiency and longest effective absorption period. The SO_2 removal efficiency is closely dependent on the basic conditions during the preparation process of the SO_2 absorbent. The SO_2 absorption activity increased with the reaction temperature and reached a maximum at 120^oC for fly ash and 130^oC for both bottom ash and slag. Maximum SO_2 removal efficiency was also attained by fly ash at 10 hour curing period. Bottom ash and slag had high activity at 15 - 20 hours of curing time. CaO content in the range of 20 ~ 30% will give a high SO_2 absorption activity.

I. Introduction

The clamor for environmental protection is a global concern. With increasing economic and social activities, degradation of the environment due to increased energy demand is inevitable. As oil resource is fast becoming depleted, dependence on coal and other solid fuels will have to be resorted to. However, reduction of air pollutants such as SO_2, NO_x, and CO_2 emissions during the combustion of these fuels is already a major concern for advanced countries. In the Philippines, the government has started to imposed environmental regulations to keep its environment free from hazardous and toxic elements. Among the detrimental pollutants being looked into, the government is focusing its attention to the hazardous emissions from coal-fired power plants, in particular, to the reduction of SO_2 emissions.

The Industrial Technology Development Institute (ITDI) of the Department of Science and Technology (DOST) through the Fuels and Energy Division (FED) has entered into a joint collaboration with the Hokkaido National Industrial Research Institute (HNIRI), Agency of Industrial Science and Technology (AIST), Ministry of International Trade and Industry (MITI), Japan to conduct a research study on the preparation of highly active absorbent for SO_2 removal from coal ash.

At present, the Philippines has four (4) existing coal-fired thermal power plants located in Calaca, Batangas, Cebu and Pagbilao, Quezon with a total of rated capacity of 1441 MW. These power plants generate about 1 million metric ton of ash per year. At present, these plants do not have a means for controlling sulfur emissions. Adapting technologies such as the application of absorbent for SO_2 removal from coal ash could minimize the environmental impact on the operation of coal-fired power plants.

II. Materials and Methods

2.1 Raw Materials

Coal ash samples used in the experiments were collected from Batangas Coal-Fired Thermal Power Plant. The limestone was obtained from a cement plant in Norzagaray, Bulacan.

2.2 Chemical Composition

The chemical compositions of the coal ash samples and the Philippine limestone were determined by atomic absorption spectrometry.

2.3 X-ray Powder Diffraction Analysis

The mineralogical composition of the coal ash samples, Philippine limestone and SO_2 absorbents were determined by the use of a Rigaku- X-ray Diffractometer Model HV21. The X-ray beam source was a copper tube with nickel filter. A potential of 35 kV and 20 mA current were applied at a scanning speed of 2°/min.

2.4 Morphological Analysis

SEM photographs of the coal ash samples and the SO_2 absorbent were taken on a JEOL Scanning Electron Microscope Model JSM-TSO with an accelerating voltage of 5 kV for the samples coated with gold by ion spattering.

2.5 Thermal Analysis

Thermal analysis of Philippine limestone was conducted using a Rigaku Thermoflex unit α-Al_2O_3 as reference sample. The limestone sample was heated up to $1000^{\circ}C$ at a heating rate of 10°/min under air atmosphere, TG range at full scale of 100% and DTA range of ± 100 uV.

2.6 Preparation of the SO_2 Absorbent

Absorbents were prepared using calcium carbonate and coal ash. For the preparation of 100g absorbent $CaCO_3$ (CaO: 5~45 wt %) was added to coal ash (55~95 wt%). Water and carbon dioxide (CO_2) were added. The resulting slurry was then cured with constant stirring in a curing vessel at 120°C for 2~20 hours. The cured absorbents were then filtered and dried at 200°C for 2 hours. The dried absorbents were crushed to 1~2 mm particle size and screened to remove the smaller particles. The basic conditions needed and schematic diagram for the preparation of the SO_2 absorbent are given in Table 1 and Figure 1, respectively.

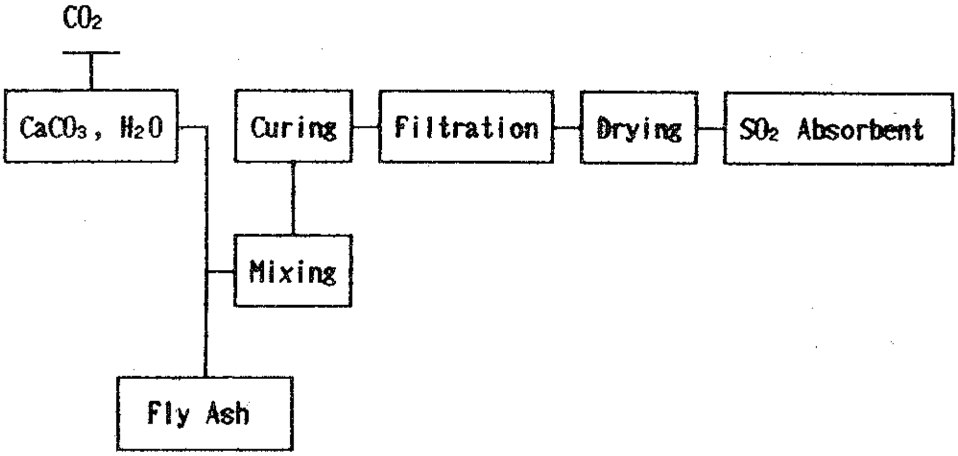

Figure 1. Preparation process of SO_2 absorbent

Table 1

Basic Conditions for the Preparation of SO_2 absorbent.

Combination of raw materials	Coal ash: 55 ~ 95 wt% CaO ($CaCO_3$): 5 ~ 45 wt%
Curing condition	Reaction temperature: 120°C Reaction time: 2 ~ 20 hrs.
Drying temperature: 200 °C	Drying time: 2 hrs.

2.7 SO_2 Absorption Test

The removal efficiency of the SO_2 absorbent was determined using the experimental SO_2 Absorption Analyzer shown in Figure 2. The absorbent was placed in a sample holder enclosed in a furnace and heated to 165°C. The temperature was measured by a thermocouple. Simulated flue gas mixture composed of SO_2, NO, H_20 and N_2 as the balance gas, flows to the reactor at a space velocity (SV) of 162 h^{-1}. Gas leaks were monitored through a pressure drop in the manometer. The tested gas was passed through a moisture remover before going to the gas analyzer. The absorption conditions used throughout the experiment were: 900 ppm SO_2; 450 ppm NO; 13% CO_2; 6% O_2; 10% H_2O; temperature: 165°C and SO_2 absorbent weight of 5 grams.

The effects of curing temperature, curing time and percent CaO of the absorbent on the SO_2 removal efficiency were determined using the experimental SO_2 Analyzer.

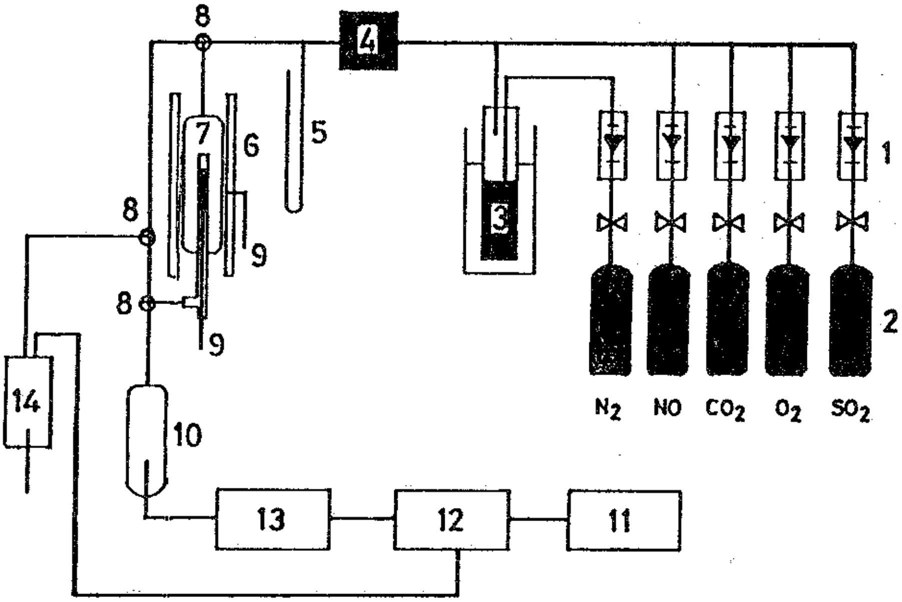

Figure 2. Experimental Set-Up of the SO2 Absorption Analyzer

1. Flowmeter	8. Cock
2. Gas cylinder	9. Thermocouple
3. Steamer	10. Moisture remover
4. Gas mixer	11. Gas sampling unit
5. Manometer	12. Analyzer (SO_2, NO, CO_2. O_2)
6. Furnace	13. Recorder
7. Sample holder	14. Scrubber

III. Results and Discussion

3.1 Chemical Composition

The chemical composition of the coal ash samples is given in Table 2. It can be seen from the table that the coal ash samples contain large amounts of α-SiO_2 (quartz), and Al_2O_3 (alumina) and small amounts of Fe_2O_3 (hematite), CaO (lime) and MgO (periclase). A minor trace element of K_2O is also present in very small amount. The coal ash samples contain total carbon ranging from 4.02 to 11.0%. Sulfur content for all the coal ashes is very low ranging from 0.07 to 0.17%.

Based on the classification established by Voina and Todor [5] which considers the ratio between SiO_2 and SO_3, the Philippine coal ashes are of the silico-aluminous type with $SiO_2/Al_2O_3 < 2$ and $CaO < 15\%$.

Table 2
Chemical Composition of Coal Ash

Composition %	Fly ash	Bottom ash	Slag
SiO_2	47.07	48.66	48.07
Al_2O_3	30.01	24.83	26.12
Fe_2O_3	4.87	7.89	7.92
CaO	4.50	5.89	6.47
MgO	1.37	1.81	1.6
K_2O	0.79	0.77	0.63
S	0.16	0.17	0.07
C	6.32	11.00	4.02

3.2 Morphological Analysis of the Coal Ash Samples

Shown in Figure 3 are the SEM photomicrographs of the coal ash samples. The photomicrograph of fly ash reveals an abundance of smooth-surfaced spherical particles with varying sizes. The irregular shaped particle may be coal fragment that did not fully burn during the combustion process. The photomicrograph of bottom ash shows the deposition of small spherical particles on surfaces. The photomicrograph of slag shows that it consists mainly of large non-spherical particles that were "rock-like".

3.3 X-ray Powder Diffraction Analysis

Shown in Figure 4 is the X-ray diffraction profile of the coal ash samples. It can be noted that fly ash and bottom ash consist mainly of α-SiO_2 (quartz), $3Al_2O_3SiO_2$ (mullite), α-Fe_2O_3 (hematite), CaO (lime), $CaSiO_3$ (wollastonite), α-Al_2O_3 (corundum) and some minor elements. Slag, on the other hand, contains traces of $CaAl_2Si_2O_8$ (plagioclase).

Shown in Figure 5 is the X-ray diffraction pattern for Philippine limestone and $CaCO_3$ Guaranteed Reagent, 99.9% min. purity. It can be observed that the calcite content of Philippine limestone is comparable to the calcite content of the $CaCO_3$ Guaranteed Reagent (minimum 99.9% after drying at 110°C).

3.4 Thermal Analysis

Figure 6 shows the thermograph obtained for the Philippine limestone. The thermogravimetric (TG) curve depicts total weight loss while differential thermal analysis curve shows if a phase undergoes a change or decomposition with gain or loss of heat during the heating up of the material. The TG curve shows that limestone starts to lose weight at about 550°C. The peak at 794°C maybe attributed to impurities present in the sample while the peak at 823°C indicates the decomposition temperature of Philippine limestone.

3.5 SO_2 Absorption Characteristics of Absorbent

The addition of CO_2 and H_2O during the preparation process for the SO_2 absorbent result in the formation of ions as shown in the following reaction:

$$CaCO_3 + CO_2 + H_2O \longrightarrow Ca^{++} + 2HCO_3^-$$

$$Ca^{++} + 2HCO_3^- + \text{Coal Ash} \longrightarrow Ca \cdot Al \cdot \text{Silicate} \cdot \text{Hydrate}$$

With the addition of coal ash, Ca^{++} reacts with the non-crystalline components of coal ash like SiO_2 and Al_2O_3. The produced absorbent reacts with SO_2 to form ettringite [$Ca_6Al_2(SO_4)_3(OH)_{12}\cdot 25H_2O$ or $6CaO\cdot Al_2O_3\cdot 3SO_3\cdot 31H_2O$] and $CaSO_4$.

Figure 7 shows the absorption curve of the three coal ash samples. Among the coal ashes, fly ash has the highest SO_2 removal efficiency and longest effective SO_2 absorption time at 96 ~ 98% and 4 hours, respectively. Beyond 4 hours, the SO_2 absorbent from fly ash lost its activity for absorption. It could also be observed that SO_2 removal efficiency for both bottom ash and slag were very low of short duration.

3.6 Effect of Varying Curing Temperature on SO_2 Removal Efficiency

Figure 8 shows the correlation between curing temperature and SO_2 removal efficiency. It can be observed that the curing temperature for coal fly ash to obtain the maximum removal efficiency of 96 ~ 98% is at 120°C. At this curing temperature however, bottom ash and slag only registered about 30% and 10% SO_2 removal efficiency, but increasing the reaction temperature will give a slight increase on their SO_2 absorption capacity.

3.7 Effect of Varying Curing Time on SO_2 Removal Efficiency

Figure 9 shows that the activity for SO_2 absorption increased with curing time from 5 ~ 10 hours. This could be attributed to an increase in the surface area of the absorbent. For coal fly ash, the curing time to get maximum SO_2 removal efficiency of 98% is at 10 hours. However, increasing the curing time beyond 15 hours will result to a decrease in the activity of the absorbent for the SO_2 removal. At 10 hours of curing time, bottom ash and slag obtained 30% and 10% SO_2 removal efficiency. Increasing the curing period will give a slight increase on their SO_2 absorption activity.

3.8 Effect of Varying CaO Content (%) on SO_2 Removal Efficiency

Figure 10 shows the variation of the SO_2 removal efficiency as a function of the CaO content of the absorbent. The SO_2 removal efficiency markedly increase with an increase in the CaO content and reached a maximum at CaO content ranging from 20 ~30%. However, above 30% CaO content, the activity for SO_2 absorption drastically decreased and the absorbent starts to lose its activity. A very high CaO content in the presence of non-crystalline components in great quantities in coal ash results in the formation of $Ca(OH)_2$. When exposed to air, $Ca(OH)_2$ is converted to $CaCO_3$ which has no reaction with SO_2.

3.9 Morphological Structure of the SO_2 Absorbent

The microstructure of the SO_2 absorbent as shown in Figure 11 is very much different from the raw materials. It reveals some "needle-like" and crystal flake structures.

3.10 Comparison of the X-ray Diffraction Profile of the SO_2 Absorbent and Spent SO_2 Absorbent

The x-ray diffraction pattern of SO_2 absorbent and spent SO_2 absorbent are shown in Figure 12. In the SO_2 absorbent, the peaks attributed to $Ca(OH)_2$ formed from the reaction of some $CaCO_3$ with water appeared at (2θ = 34.0, 18.1, 47.0, 50.8, 64.3). It could be observed however, that the intensity of the peaks for $Ca(OH)_2$ apparently decreased in the spent SO_2 absorbent.

In the spent SO_2 absorbent, some new peaks were formed at (2θ = 15.8, 22.9, 35.0). This indicated the presence of ettringite [$Ca_6Al_2(SO_4)_3(OH)_{12} \cdot 25H_2O$ or $6CaO \cdot Al_2O_3 \cdot 31H_2O$]. The peaks at ($2\theta$ = 25.4, 31.3, 38.6, 40.9, 48.7) were known to be $CaSO_4$.

IV. Conclusions

The emissions of air pollutants in particular SO_2 and NO_x from coal-fired thermal power plants could be reduced by a practical desulfurization system such as the preparation of highly active SO_2 absorbent from coal ash.

Based on the results of this study, the following conclusions could be drawn:

1. The chemical and mineralogical composition of the Philippine coal ash and limestone indicated that they can be utilized as raw materials for the preparation of highly active absorbent for SO_2 removal.
2. Among the three coal ashes fly ash, bottom ash and slag, fly ash showed the highest SO_2 removal efficiency and longest effective SO_2 absorption time.
3. The best conditions for the preparation of SO_2 absorbent from fly ash to obtain maximum activity for SO_2 removal is at curing temperature of 120°C and curing time of 10 hours. For both bottom ash and slag, curing temperature at 130°C and curing time of 15~20 hours will increase their SO_2 removal efficiency.
4. To obtain a highly active SO_2 absorbent, the CaO content should be in the range of 20 ~30%.
5. The spent SO_2 absorbent could still be used as a raw material in the preparation of highly active absorbent for SO_2 removal. However, in this case, another method of preparation shall be employed using calcium oxide, calcium sulfate (from spent SO_2 absorbent) and coal fly ash as the raw material.

References

1. MacCarthy, G.J. Glasser, F.P., Roy, D.M., Diamond, S. (1984). Fly Ash and Coal Conversion By-Products; Characterization, Utilization and Disposal I and III, Symposia Proceedings, Materials Research Society, Massachusetts, U.S.A.
2. Pugal, D.L. Herrera, A.B., et.al. "Studies on the Fusibility of Coal Ash", Philippine Engineering Journal, Vol. XVI, No.1, June 1995, pp. 85 -102
3. Oscik, J. (1982). Adsorption, John Wiley & Sons, New York.
4. Tsuchiai, H., Ishikuza, T. Ueno, T. (1995). "Highly Active Absorbent for SO_2 Removal Prepared from Coal Fly Ash", Industrial and Engineering Chemistry, Research, January 1995.
5. Voina, N.I., Todor, D.N. (1978). Thermal Analysis of Coal and Coal Products, Vol. 11, Academic Press, Inc.

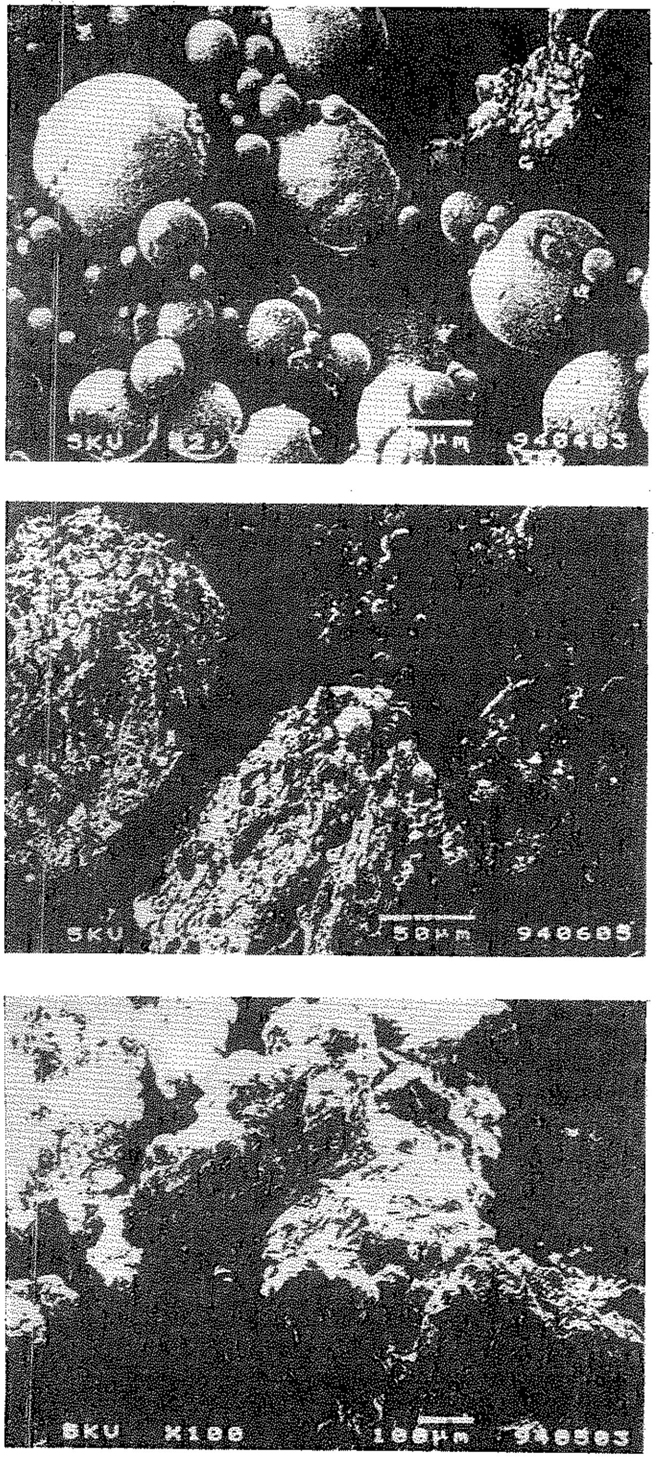

Fly ash

Bottom Ash

Slag

Figure 3. Scanning Electron Micrographs of Coal Ash

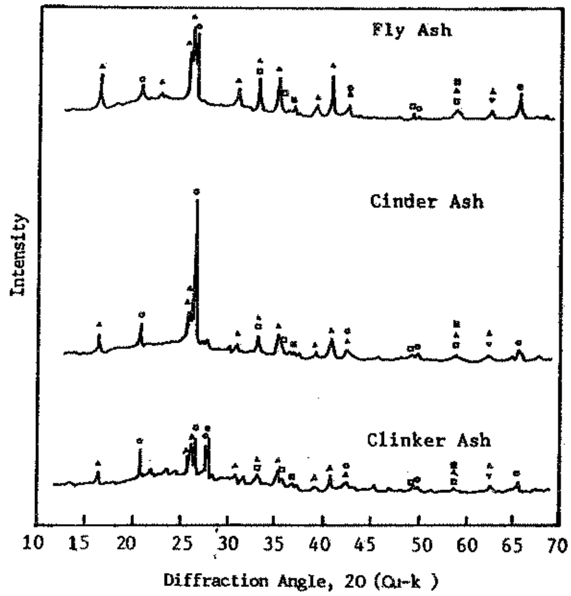

Figure 4. X-ray Diffraction Pattern of Coal Ash

o : α-SiO_2, Δ : $Al_2O_3 \cdot 2SiO_2$, ▯ : α-Fe_2O_3,
● : $CaAl_2Si_2O_3$, ▲ : $CaSiO_3$, ■ : CaO, ∇ : α- Al_2O_3

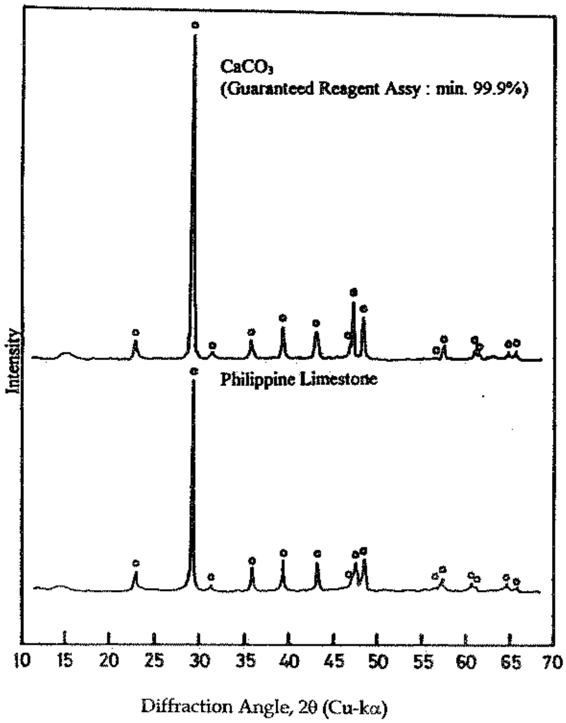

Figure 5. X-ray Diffraction Pattern of Limestone

o : $CaCO_3$ (Calcite)

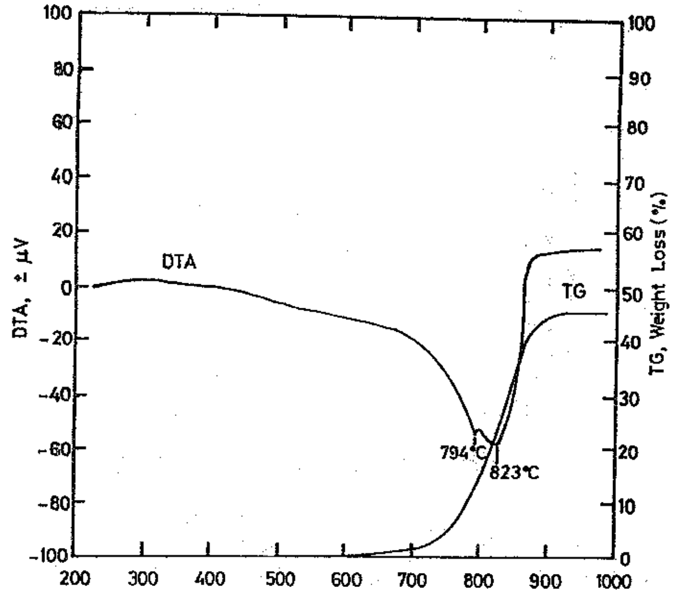

Figure 6. Thermal Analysis of Philippine Limestone

Ref. Sample: α- Al_2O_3
Program rate: 10°C/min
Atmosphere: air

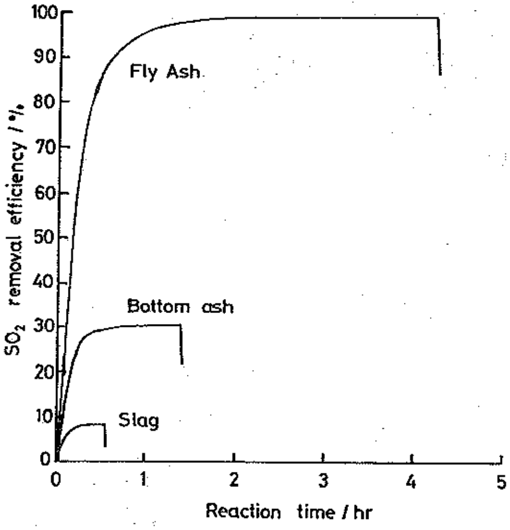

Figure 7. SO_2 absorption characteristics of SO_2 absorbent

Curing time: 10 hrs, Curing temperature: 120°C
Absorption condition
SO_2:900 ppm, NO:450 ppm, CO_2: 13%, O_2:6%, H_2O:10%,
Reaction temperature: 165°C

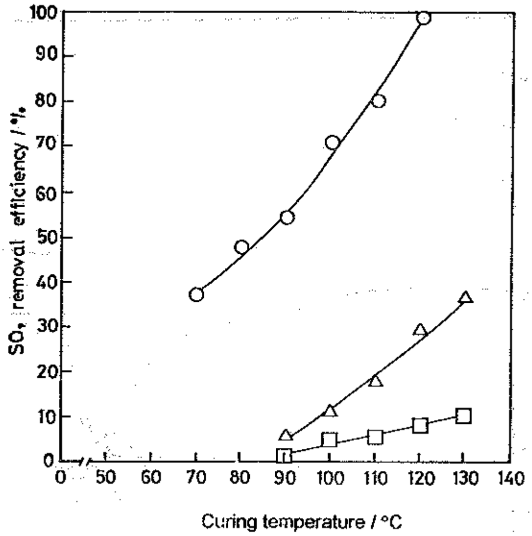

Figure 8. Correlation between curing temperature and SO_2 removal efficiency

Curing time: 10 hrs
Absorption condition
SO_2:900 ppm, NO:450 ppm, CO_2:13%, O_2:6%, H_2O:10%
Reaction temperature: 165 °C
O : Fly ash, Δ: Bottom ash, □ : Slag

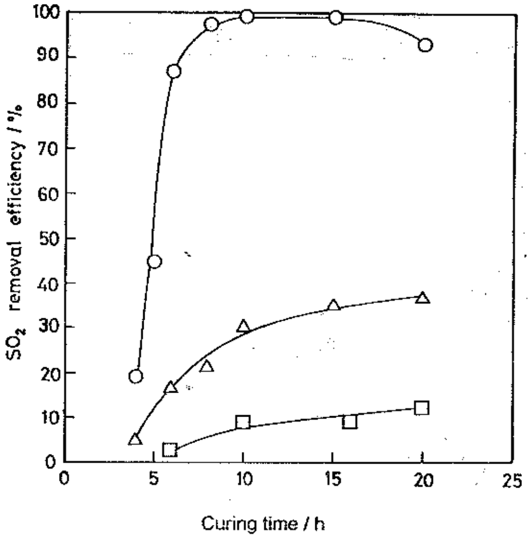

Figure 9. Correlation between curing time and SO_2 removal efficiency

Curing temperature: 120°C
Absorption condition
SO_2:900 ppm, NO:450 ppm, CO_2:13%, O_2:6%, H_2O:10%
Reaction temperature: 165 °C
O : Fly ash, Δ: Bottom ash, □ : Slag

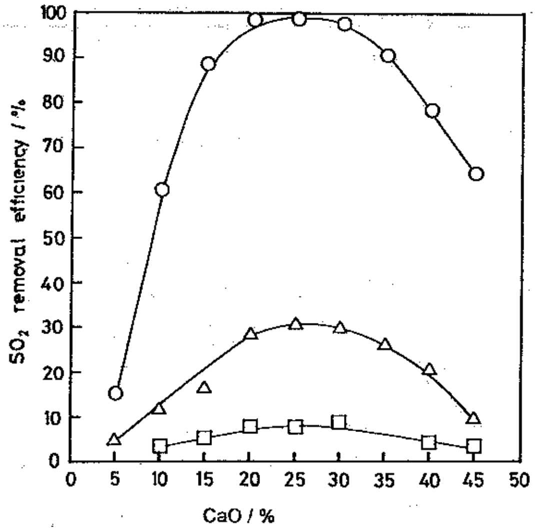

Figure 10. Correlation between CaO content and SO2 removal efficiency

Curing temperature: 120°C
Absorption condition
SO_2:900 ppm, NO:450 ppm, CO_2:13%, O_2:6%, H_2O:10%
Reaction temperature: 165 °C
O : Fly ash, Δ: Bottom ash, □ : Slag

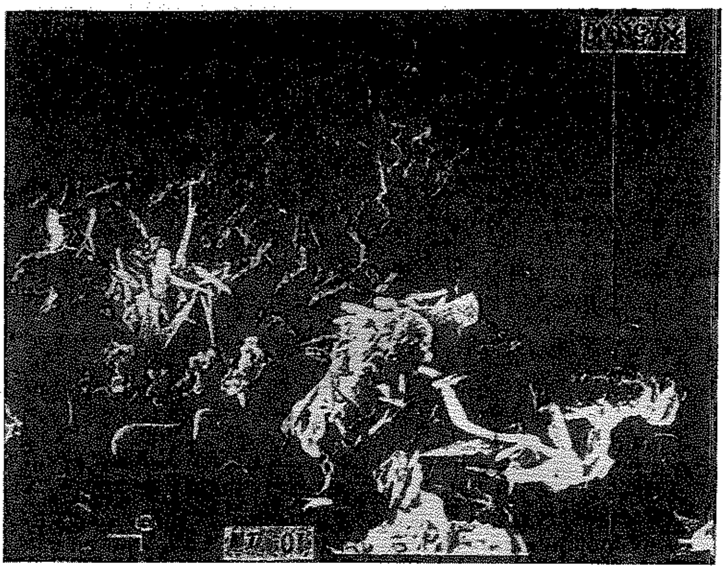

Figure 11. Scanning Electron Micrographs of SO2 Absorbent

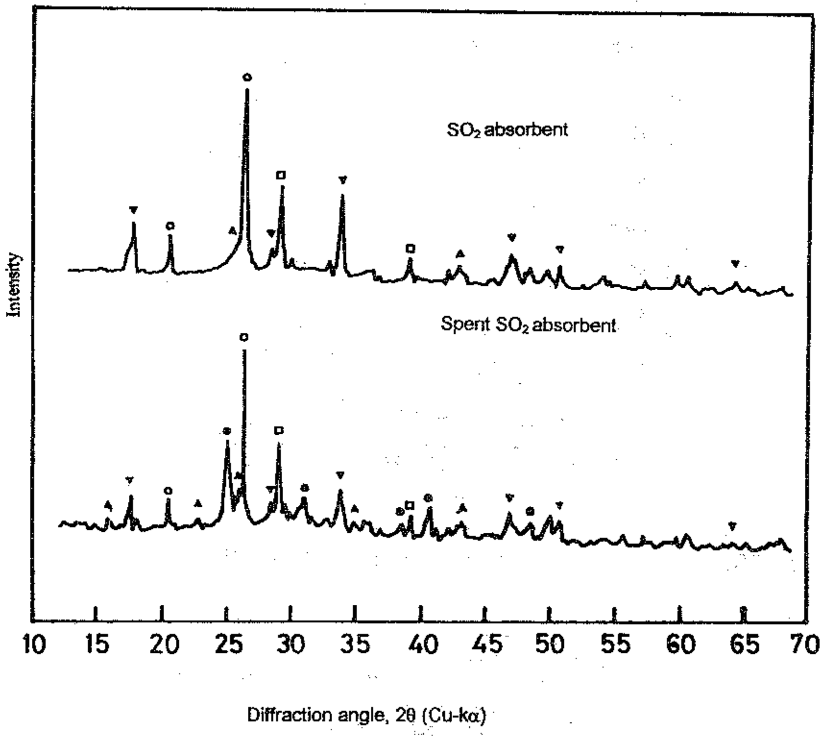

Figure 12. X-ray diffraction pattern of SO_2 absorbent and spent SO_2 absorbent

O : α - SiO_2, Δ : $3Al_2O_3 \cdot 2SiO_2$, □ : $CaCO_3$, ● : $CaSO_4$,
▲ : $Ca_6Al_2(SO_4)_3(OH)_{12} \cdot 25H_2O$ or $6CaO \cdot Al_2O_3 \cdot 3SO_3 \cdot 3H_2O$
▽ : $Ca(OH)_2$